Design and PIL Test of High Performance MPPT Controller Based on P&O-Backstepping Applied to DC-DC Converter

Omar Diouri [1,*], Ahmed Gaga [2], Saloua Senhaji [3], Mohammed Ouazzani Jamil [4]
[1, 2, 3, 4] Laboratory of Intelligent Systems, Energy and Sustainable Development, Private University of Fez - UPF, Fez, Morocco
[2] Laboratory of Physics and Engineering Sciences, Research team in Embedded Systems Engineering, Automation, Signal, Telecommunications and Smart Materials, Department of Physics, Polydisciplinary Faculty, Sultan Moulay Sliman University - USMS, Beni-Mellal, Morocco
Email: [1] diouri@upf.ac.ma, [2] gaga.ahmad@gmail.com, [3] senhaji@upf.ac.ma, [4] ouazzani@upf.ac.ma,
*Corresponding Author

Abstract—**This paper presents the design, test and validation process of the maximum power point tracking (MPPT) based on the Perturb and Observe backstepping controller. The design of this robust controller follows a sequence of two tests of the validated model-based design (MBD) approach. Our contribution is to give a roadmap for designing, testing and validating embedded software for MPPT algorithms. Perturb and observe algorithm is used to generate the reference voltage which is used by the backstepping controller to generate the maximum power. Then, after simulation of all these techniques, generated optimized C code for the STM32F4 microcontroller is necessary to test the controller on embedded platform. Therefore, the algorithm of MPPT is simulated by Model in the Loop (MIL) and Processor in the Loop (PIL) techniques. The results show that the proposed system has full control over reference power, for different atmospheric changes, by backstepping and integrating into a 32-bit ARM microcontroller. In all of the various tests, the embedded software developed demonstrates high compliance and high performance with MPPT requirements.**

Keywords—MPPT algorithm; P&O backstepping; PIL test; MIL test; Boost converter

I. INTRODUCTION

Solar energy is one of the most widely used green energy technologies because it is clean, inexhaustible and inexpensive. It can be controlled and monitored by new technology as a machine learning and the Internet of Things [1]–[6]. DC-DC converters are available in a variety of topologies [7]–[11]. In this task, a boost converter is used to track the MPP and achieve the desired input voltage value for adjusting the output voltage of the solar panel according to specifications. The main goal of boost converters is to use MPPT technology to enable PV arrays to generate the maximum power possible [12]–[15].

There are many algorithms for efficiently tracking MPPs. Some academic papers describe two types of MPPT techniques. Indirect MPP monitoring such as fractional open circuit voltage technology [16] and direct MPP tracking such as incremental conductance [17]–[22] or perturb and observe (P&O). Used in this study. There are other research papers focusing on fuzzy logic algorithms for controlling MPPT [23]. The PV curve has a reducing nature to the right of the MPP and an increasing nature to the left of the MPP, so this P&O algorithm takes advantage of that [24], [25]. The disadvantage of this algorithm is that the operating point at the MPP is never smooth and steady. It is constantly oscillating in the MPP field [26]–[28]. To minimize this, we can use small disturbance changes around the MPP.

Another weakness is that the output voltage of the DC-DC converter cannot be controlled. Our proposed system is the Backstepping control with P&O blocks can be used to generate the reference voltage monitored by the controller [29]. In addition, boost converter control ensures that the PV generator supplies the same voltage as the MPPT block. Much research has focused on backstepping control because of its ability to design stability controls for nonlinear dynamic systems [30], [31]. The designer's goal is usually to find a positive deterministic function called the "Lyapunov candidate function" [32]. The derivative of this function is limited to a negative deterministic function using the system input [33], [34]. However, the hardware implementation is difficult, especially the implementation of backstepping controller. However, when starting a hardware implementation of the MPPT algorithm on a digital device such as a microcontroller, FPGA, DSP, etc., sometimes there is discrepancies that may occur between the software and the requirements during the development process [35], [36]. Therefore, when an error occurs, it is difficult to know exactly which component is causing the error. This can increase the time it takes to debug run-time errors. Therefore, in other areas such as aviation and automotive, software can be generated from models tested by simulation, and for implementing, there are various steps between simulation and hardware implementation [37], [38]. In addition, the choice of such MPPT algorithms is based on their tracking speed, steady-state performance and the ability to be implemented on embedded boards that ensure high robustness. Therefore, the most commonly used P&O and INC algorithms [39]. The MPPT implementation step, on the other hand, is required to validate the algorithm under variation of temperature and radiation conditions [40].

Due to the random fluctuations in atmospheric conditions, PV modules cannot reproduce the desired power. Therefore, photovoltaic panel simulators are often used instead of real PV panels [41]. The main objective of [42] implemented a modified incremental conductivity MPPT algorithm using the Agilent solar array simulator. PV emulators with DC power supplies have also been proposed [43], [44]. However, PV array simulators or DC power supplies are expensive equipment and are not always available. Therefore, the PIL test is considered as a low cost solution for testing the hardware implementation of the maximum power algorithm under a variety of solar and temperature conditions.

II. Validating in Model Based Design

To transform the development of complex systems, market-leading companies are adopting the Model-Based Design MBD approach by systematically using models throughout the process. Model-Based Systems Engineering (MBSE) is abofiguut using models to support the complete system life cycle. Simulink links system requirements and architecture to detailed component design, implementation, and testing in the development process.

This technique is also proactive because it gives us an opportunity to verify and check the interaction of system components and interfaces before implementing the hardware. In addition, test the software with a real-time embedded controller without implementing the entire system. Taking the next step and validating the phases means that the software will be more accurate and mature. This increases the reliability of the designed software. In this research, this technique involves two main validation steps: model-in-the-loop (MIL) and processor-in-the-loop (PIL) [45]–[47].

The goal of the MIL test is to validate the model function against either the algorithmic requirements or the reference model. That is, prepare a test case for the model under test and check if the model meets the requirements.

The PIL validation process is an important part of the design cycle to ensure that the deployment code behaves as designed and is bug-free when implemented on the target. During this time, the embedded target C code runs separately from the plant system that continues to run on the host computer. In addition, processor-in-the-loop (PIL) simulation provides a way to bridge the gap between simulation and final system design [48]. This tool enhances and provides the realism of numerical simulation Access to other hardware features (see Fig. 1).

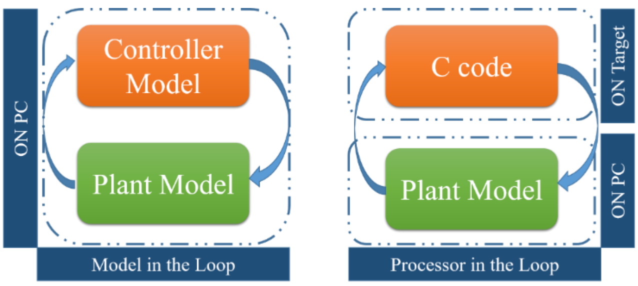

Fig. 1. Block diagram of MIL and PIL test

III. System Description

The block diagram of the PV structure is shown in Fig. 2. It consists of two main components: a power electronics converter and a photovoltaic array. This converter is powered by backstepping controller in order to provide full power to the load. The converter is a DC-DC boost that tracks the maximum electrical energy provided by the PV array for different values of irradiance and temperature. Generates a reference voltage for the backstepping block to force the PV array to supply that voltage.

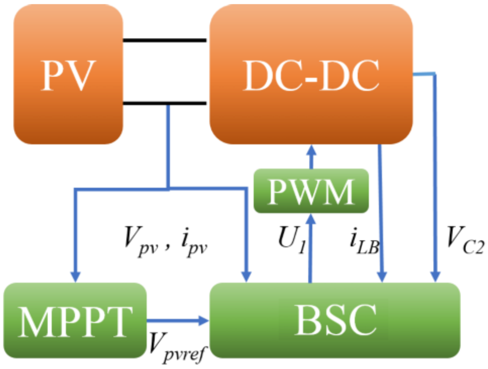

Fig. 2. Bloc diagram of boost converter with P&O-backstepping controller

A. PV Array

The conversion of photons to electricity using semiconductor materials is the concept behind photovoltaic radiation. A photovoltaic generator consists of several solar cells. The basic part is a solar cell that can only produce a few watts. As a result, the PV system uses solar panels consisting of multiple solar cells connected in parallel and in series to maximize current and voltage, respectively. The model parameters of PV array are shown in Fig. 3 and curves of I-V and P-V in Fig. 4.

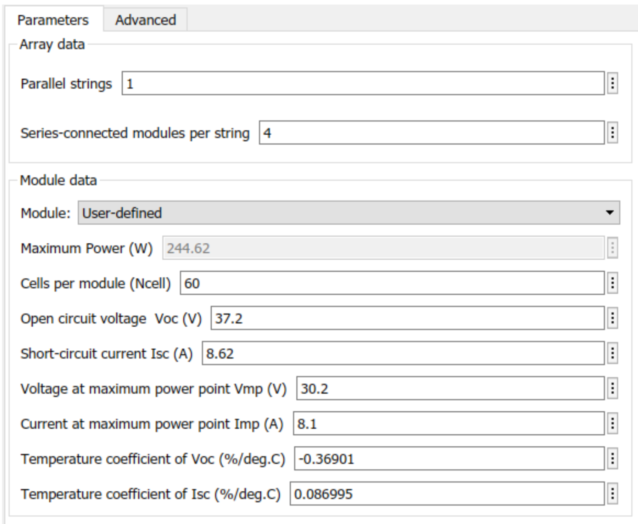
Parameters | Advanced

Array data

Parallel strings	1
Series-connected modules per string	4

Module data

Module:	User-defined
Maximum Power (W)	244.62
Cells per module (Ncell)	60
Open circuit voltage Voc (V)	37.2
Short-circuit current Isc (A)	8.62
Voltage at maximum power point Vmp (V)	30.2
Current at maximum power point Imp (A)	8.1
Temperature coefficient of Voc (%/deg.C)	-0.36901
Temperature coefficient of Isc (%/deg.C)	0.086995

Fig. 3. Model parameters of PV array

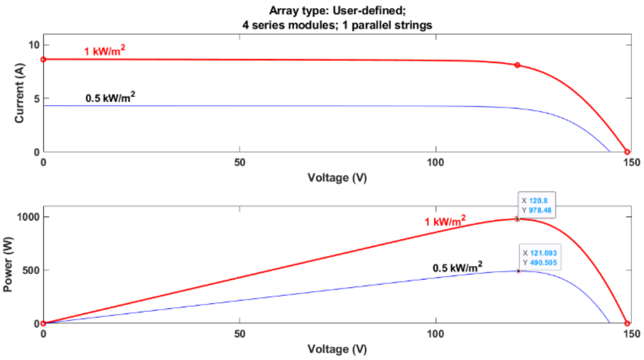

Fig. 4. I-V and P-V Curves of PV for 1000 and 500 W/m2 of irradiance

B. MPPT P&O Algorithm

There is one outlet known to be the most powerful MPP. The PV array produces the highest possible power and can be tracked using a special algorithm called Maximum Power Point Tracking (MPPT). In this study, a P&O algorithm is applied to the PV array voltage to increase or decrease the power as shown in Fig. 5.

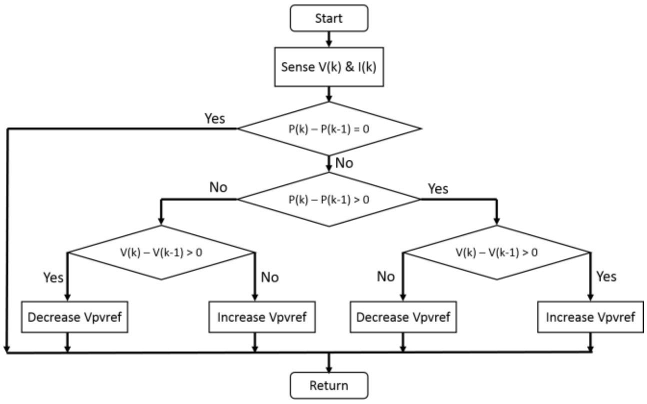

Fig. 5. Flowchart of perturb and observe

C. Boost converter

There are various types of DC-DC converters in the literature that can convert one voltage level to another. Boost and buck converters are two examples [49], [50]. The second block after the PV array is a simple boost DC-DC converter that boosts the voltage from the low input voltage of the PV array to the high load output voltage. To get the MPP in different atmospheric environments, connect the input of the boost converter to the PV array. Fig. 6 shows the circuit block of a DC-DC converter with the backstepping. This controller can use a PWM generator to provide the appropriate duty cycle and control the power transistors of the boost converter. Fig. 6 shows a schematic diagram of the boost converter used in this study. Which ipv and Vpv are the two parameters produced by the PV array depending on the current and voltage, respectively. C1 and C2 are the input capacitor and output capacitor of the boost converter, respectively, and LB is the boost inductance. VC2 represents the system output voltage and iLB represents the inductor current.

IV. Design of MPPT Backstepping Control

Using the Kirchhoff theorem on the boost model seen in Fig. 6, (1) and (2) reflect the boost's dynamic model:

$$C_1 \frac{dV_{pv}}{dt} = i_{pv} - i_{LB} \tag{1}$$

$$L_B \frac{di_{LB}}{dt} = V_{pv} - (1 - u_1)V_{C2} \tag{2}$$

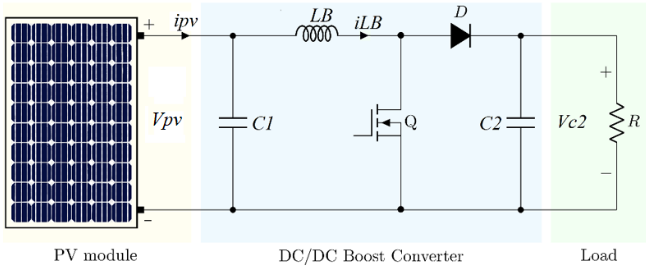

Fig. 6. Boost converter

Equations (1) and (2) can be rearranged as follows using the voltage V_{pv} as the system state and u_1 as the control signal for the boost converter:

$$\dot{x}_1 = \frac{1}{C_1} i_{pv} - \frac{1}{C_1} x_2 \tag{3}$$

$$\dot{x}_2 = \frac{1}{L_B} x_1 - \frac{(1 - u_1)}{L_B} V_{C2} \tag{4}$$

Where x_1 and x_2 are the average value of V_{pv} and i_{LB} respectively.

The goal is to use a back-stepping control to track the photovoltaic reference voltage in order to generate the most power from the PV array. The control law is derived from the Lyapunov dynamic systems. e_1 is the error, which is defined as:

$$e_1 = x_1 - V_{pvref} \tag{5}$$

$$\dot{e}_1 = \dot{x}_1 - \dot{V}_{pvref} = \frac{1}{C_1} i_{pv} - \frac{1}{C_1} x_2 - \dot{V}_{pvref} \tag{6}$$

V_1 is the first Lyapunov function, and it is defined as follows:

$$V_1 = 0.5 e_1^2 \tag{7}$$

$$\dot{V}_1 = e_1 \dot{e}_1 = e_1 \left(\frac{1}{C_1} i_{pv} - \frac{1}{C_1} x_2 - \dot{V}_{pvref} \right) \tag{8}$$

It is necessary to get $\dot{V}_1 = -k_1 e_1^2 < 0$ for this raison we obtain the (9), where k_1 is positive.

$$\frac{1}{C_1} i_{pv} - \frac{1}{C_1} x_2 - \dot{V}_{pvref} = -k_1 e_1 \tag{9}$$

The system's virtual control is x_2^*, which is equal to:

$$x_2^* = i_{pv} + C_1 k_1 e_1 - C_1 \dot{V}_{pvref} \tag{10}$$

Where the second error is defined as follows between the second state variable x_2 and its desired value x_2^*:

$$e_2 = x_2 - x_2^* \tag{11}$$

The derivative of error e_1 is:

$$\dot{e}_1 = \frac{1}{C_1} i_{pv} - \frac{1}{C_1} (x_2^* + e_2) - \dot{V}_{pvref} \tag{12}$$

$$\dot{e}_1 = \frac{1}{C_1} i_{pv} - \frac{1}{C_1}\left(i_{pv} + C_1 k_1 e_1 - C_1 \dot{V}_{pvref}\right) - \frac{1}{C_1} e_2 - \dot{V}_{pvref} \quad (13)$$

As a result, the two error's system equation is:

$$\dot{e}_1 = -k_1 e_1 - \frac{1}{C_1} e_2 \quad (14)$$

$$\dot{e}_2 = \dot{x}_2 - \dot{x}_2^* = \frac{1}{L_B} x_1 - \frac{(1-u)}{L_B} V_{C2} - \dot{x}_2^* \quad (15)$$

The second Lyapunov function V_2 and its derivative are:

$$V_2 = V_1 + \frac{1}{2} e_2^2 \quad (16)$$

$$\dot{V}_2 = \dot{V}_1 + e_2 \dot{e}_2 = e_1 \dot{e}_1 + e_2 \dot{e}_2 \quad (17)$$

New expression of the derivative of V_2 is given in (18) by combining (14) and (15) in equation (17).

$$\dot{V}_2 = -k_1 e_1^2 + e_2\left(-\frac{1}{C_1} e_1 + \frac{1}{L_B} x_1 - \frac{(1-u_1)}{L_B} V_{C2} - \dot{x}_2^*\right) \quad (18)$$

It is necessary to get $\dot{V}_2 = -k_1 e_1^2 - k_2 e_2^2 < 0$, where k_1 and k_2 are two positives:

$$-\frac{1}{C_1} e_1 + \frac{1}{L_B} x_1 - \frac{(1-u_1)}{L_B} V_{C2} - \dot{x}_2^* = -k_2 e_2 \quad (19)$$

The boost converter's control law corresponding to "u_1" is specified in equation (25).

$$u_1 = 1 - \frac{1}{V_{C2}}\left[x_1 - L_B \dot{x}_2^* - L_B\left(\frac{1}{C_1} e_1 - k_2 e_2\right)\right] \quad (20)$$

The u_1 is the appropriate control signal that can be used in order to control the transistor gate of boost converter.

V. RESULTS AND DISCUSSION

This section moves on to the most important phases of the embedded system project development process. That is, testing and integration of MPPT blocks, and subsequent verification that the system performs functions designed to run through a series of tests which are MIL and PIL tests. The systems parameters are mentioned in Table 1.

TABLE I. SYSTEM PARAMETERS

Parameter	Value
LB	3e-3 H
C1	100e-6 F
C2	100e-6 F
Fpwm	20 kHz
T	25 °C
Offset (MPPT bloc)	0.0005 V
Sample time	1e-6 s

A. *Model in the loop test*

In this phase, called Model in the Loop (MIL), running tests validates the mathematical model before proceeding to the development process. Therefore, the designed MPPT model is tested using the entire PV system in the same simulation environment (Simulink). Therefore, both the controller and the system model are simulated on the host computer. Fig. 7 shows a PV system that uses Model Based Design to control a boost converter and implement a P&O backstepping algorithm to extract maximum power. The law control equation is modeled in simulink by blocks of different arithmetic operations as shown in Fig. 8. Which Fig. 9 shows the results of the MIL test for a period of 0.4s. PV modules are exposed to rapidly changing solar irradiance. This amount of solar radiation initially increases sharply from 0 to 1000 W/m^2. As shown in the steady state of the first step, the PV power is 978 W, which is the maximum under standard test conditions of 1000 W/m2 and 25 ° C.

From Fig. 9, noticing that our proposed system was well following the reference power. To reach a power of 978.8W, the response time of our controller is 0.005s. After 0.1s, the chosen irradiation profile shows a decrease from 1000W/m^2 down to 500W/m^2. The generated PV power follows the reference with an error of 1.2W. Between 0.2s and 0.3s, the irradiation is stable on a value of 500W/m^2, the power Ppv perfectly follows Ppvref with weak oscillations around 490.5W due to the offset step of the P&O algorithm. At 0.3s, the solar irradiation increases from 500W/m^2 to 900W/m^2 to ensure that the algorithm has the ability to follow this chosen profile.

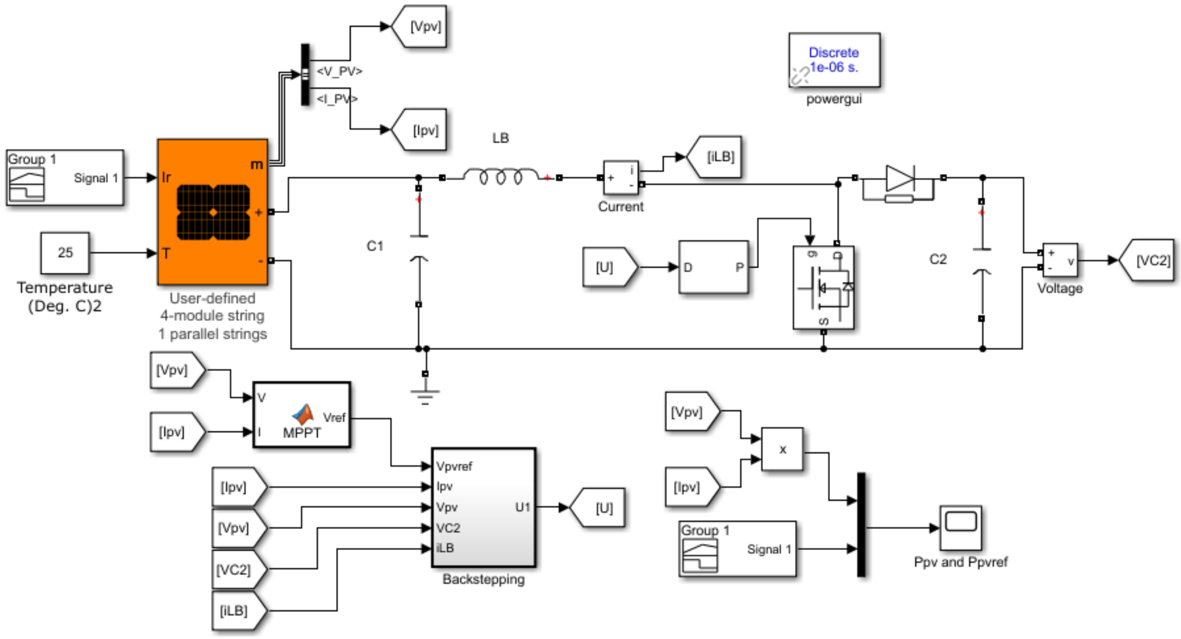

Fig. 7. PV system with backstepping control using MIL

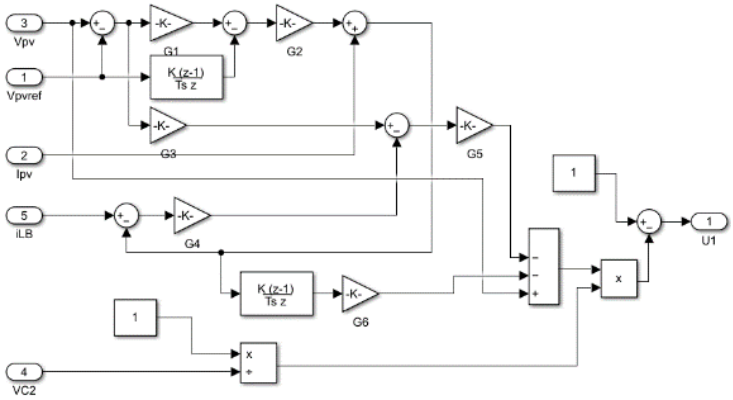

Fig. 8. Backstepping control

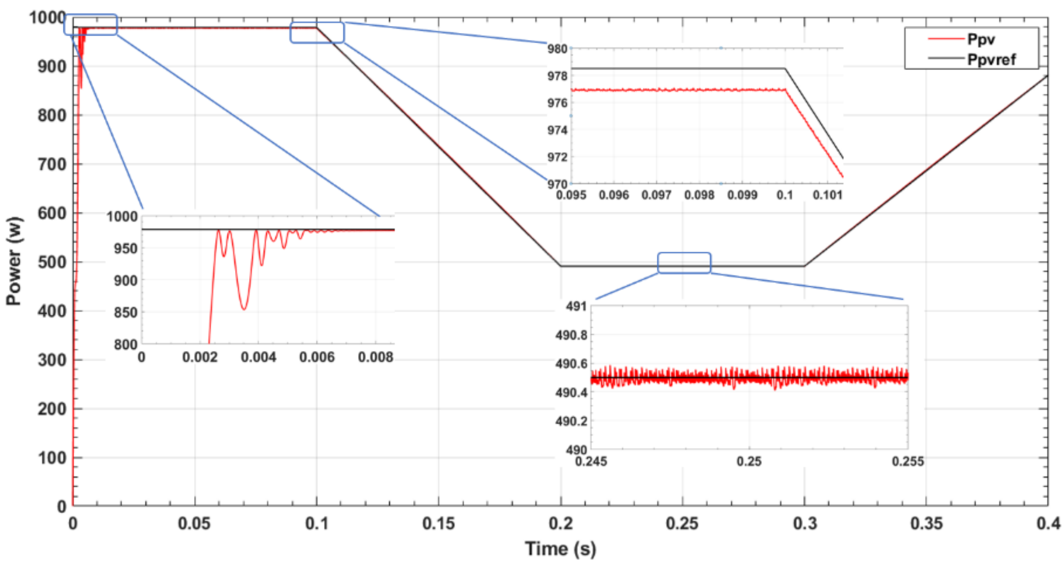

Fig. 9. PV array power generated by backstepping control using MIL test

B. Processor in the loop test

PIL testing is an important step in the development cycle to ensure that the deployment code behavior meets the requirements of the algorithm. Create a PIL block for the MPPT controller subsystem (see Fig. 10) by automatically generating a C code from a Simulink block. The STMicroelectronics STM32F4 discovery board, which is based on the ARM Cortex M4 core, will be used as the target hardware for PIL testing in this task. This low-cost board integrates a 32-bit microcontroller clocked at 168MHz, an ARM Cortex-M4 architecture capable of performing floating-point calculations. This paper used ST-Link communication, it does not require any additional device other than a USB mini-cable to connect the STM32F4 detection board to the host computer, including the Matlab / Simulink IDE. The results of Fig. 11 shows that the backstepping controller has been well verified and validated by the use of MBD because there is no difference between the two tests MIL and PIL in terms of tracking the maximum power.

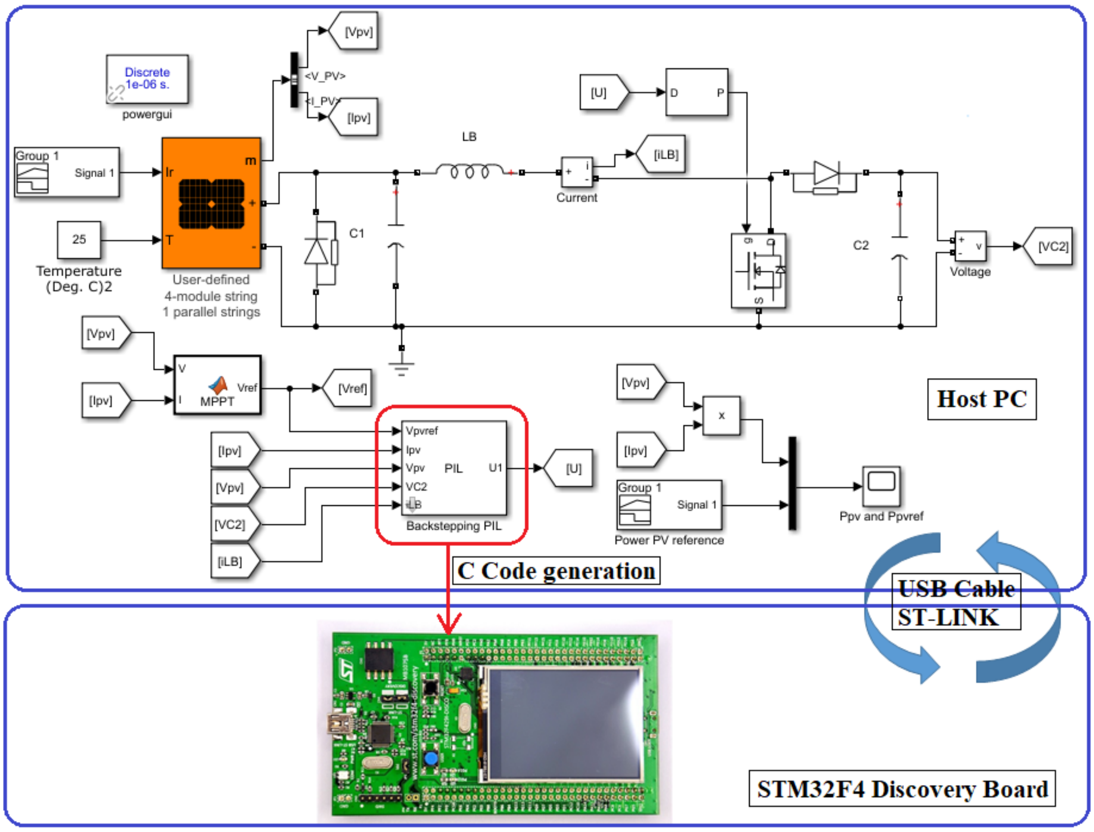

Fig. 10. PV system with backstepping control using PIL test with STM32F4 discovery board

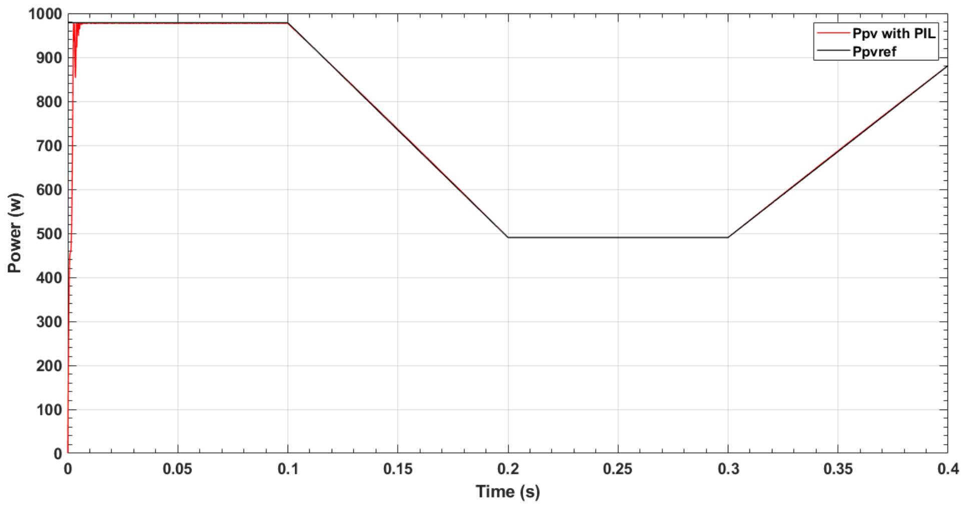

Fig. 11. PV array power generated by backstepping control using PIL

VI. CONCLUSION

This work introduces and tests a rigorous control scheme with a high power PV system based on a model-based design. We also provided a guide for developing reliable embedded MPPT controllers. MPPT control is used to optimize the solar energy provided by the PV panel. Two validation tests (MIL and PIL tests) have been passed to enhance the robustness, reliability and security levels of P&O designed using backstepping embedded software. To measure the robustness of this controller, we exposed it to sudden changes in solar irradiance. The results show that the proposed system has full control over reference power by backstepping and integrating into a 32-bit ARM microcontroller. The results obtained are Term tracking factor and speed. The PIL test validated the previous exact results obtained during the MIL test and therefore validated the MPPT requirements by finding an exact match between all tests during the development process.

ACKNOWLEDGMENT

This paper was supported by the Private University of Fez. We would like to thank the Laboratory of Intelligent Systems, Energy and Sustainable Development at UPF.

REFERENCES

[1] E. M. E. Khattabi, O. Diouri, M. Mharzi, and M. O. Jamil, "Enhancing the Energy Performance of Passive Building Through the Internet of Things," in *Artificial Intelligence and Industrial Applications*, Cham, 2021, pp. 279–286. doi: 10.1007/978-3-030-53970-2_26.

[2] A. Gaga, O. Diouri, and M. O. Jamil, "Design and realization of nano satellite cube for high precision atmosphere measurement," *Results in Engineering*, p. 100406, Apr. 2022, doi: 10.1016/j.rineng.2022.100406.

[3] H. Ouanan, O. Diouri, A. Gaga, M. Ouanan, and B. Aksasse, "A Novel Face Recognition System Based on Gabor and Zernike Features," in *Advanced Intelligent Systems for Sustainable Development (AI2SD'2019)*, Cham, 2020, pp. 9–15. doi: 10.1007/978-3-030-36677-3_2.

[4] H. Ouanan, A. Gaga, O. Diouri, M. Ouanan, and B. Aksasse, "Development of Deep Learning-Based Facial Recognition System," 2020, pp. 45–52. doi: 10.1007/978-3-030-36677-3_6.

[5] Y. Cheddadi, O. Diouri, A. Gaga, F. Errahimi, and N. Es-Sbai, "Design and Simulation of an Accurate Neural Network State-of-Charge Estimator for Lithium Ion Battery Pack', *IREACO*, vol. 10, no. 2, p. 186, Mar. 2017, doi: 10.15866/ireaco.v10i2.11957.

[6] P. Pourmaleki, W. Agutu, A. Rezaei, and N. Pourmaleki, "Techno-Economic Analysis of a 12-kW Photovoltaic System Using an Efficient Multiple Linear Regression Model Prediction," *International Journal of Robotics and Control Systems*, vol. 2, no. 2, pp. 370–378, Jun. 2022, doi: 10.31763/IJRCS.V2I2.702.

[7] M. Kasper, D. Bortis, and J. W. Kolar, "Classification and Comparative Evaluation of PV Panel-Integrated DC–DC Converter Concepts," *IEEE Transactions on Power Electronics*, vol. 29, no. 5, pp. 2511–2526, May 2014, doi: 10.1109/TPEL.2013.2273399.

[8] P. Manoharan, K. K, and S. R, "A Comparative Study and Analysis on Conventional Solar PV Based DC-DC Converters and MPPT Techniques," *Indonesian Journal of Electrical Engineering and Computer Science*, vol. 11, no. 3, Art. no. 3, Sep. 2018, doi: 10.11591/ijeecs.v11.i3.pp831-838.

[9] A. Gaga, A. Tannouche, Y. Mehdaoui, and B. E. Hadadi, "Methods for estimating lithium-ion battery state of charge for use in electric vehicles: a review," *Energy Harvesting and Systems*, Apr. 2022, doi: 10.1515/ehs-2021-0039.

[10] C. Nagarajan, K. Umadevi, S. Saravanan, and M. Muruganandam, "Performance Analysis of PSO DFFP Based DC-DC Converter with Non Isolated CI using PV Panel," *International Journal of Robotics and Control Systems*, vol. 2, no. 2, pp. 408–423, Jun. 2022, doi: 10.31763/IJRCS.V2I2.628.

[11] A. A. Rizi, A. Rezaei, M. G. Rizi, and M. A. Rizi, "Design a New Multiport DC-DC Converter to Charge an Electric Car," *International Journal of Robotics and Control Systems*, vol. 2, no. 1, pp. 87–96, Feb. 2022, doi: 10.31763/IJRCS.V2I1.566.

[12] A. Gaga, O. Diouri, N. Es-sbai, and F. Errahimi, "Design and realization of an autonomous solar system," *IOP Conf. Ser.: Mater. Sci. Eng.*, vol. 186, p. 012031, Mar. 2017, doi: 10.1088/1757-899X/186/1/012031.

[13] R. Ayop and C. W. Tan, "Design of boost converter based on maximum power point resistance for photovoltaic applications," *Solar Energy*, vol. 160, pp. 322–335, Jan. 2018, doi: 10.1016/j.solener.2017.12.016.

[14] Y. L. Chuang, M. Herrera, and A. Balal, "Using PV Fuzzy Tracking Algorithm to Charge Electric Vehicles," *International Journal of Robotics and Control Systems*, vol. 2, no. 2, pp. 253–261, Mar. 2022, doi: 10.31763/IJRCS.V2I2.636.

[15] A. Atoui, F. Akel, M. S. Boucherit, and K. Benmansour, "An Effective Low Cost Implementation of Adaptive Fuzzy Logic Based Indirect MPPT Method Using ARDUINO DUE Board," in *Artificial Intelligence and Heuristics for Smart Energy Efficiency in Smart Cities*, Cham, 2022, pp. 285–294. doi: 10.1007/978-3-030-92038-8_29.

[16] J. Ahmad, "A fractional open circuit voltage based maximum power point tracker for photovoltaic arrays," in *2010 2nd International Conference on Software Technology and Engineering*, Oct. 2010, vol. 1, pp. V1-247-V1-250. doi: 10.1109/ICSTE.2010.5608868.

[17] S. Motahhir, A. El Hammoumi, and el ghzizal Abdelaziz, "Photovoltaic system with quantitative comparative between an improved MPPT and existing INC and P&O methods under fast varying of solar irradiation," vol. 4, pp. 341–350, Nov. 2018, doi: 10.1016/j.egyr.2018.04.003.

[18] Y. Cheddadi, F. Errahimi, and N. Es-sbai, "Design and verification of photovoltaic MPPT algorithm as an automotive-based embedded software', *Solar Energy*, vol. 171, pp. 414–425, Sep. 2018, doi: 10.1016/j.solener.2018.06.085.

[19] H. M. A. Alhussain and N. Yasin, "Modeling and simulation of solar PV module for comparison of two MPPT algorithms (P&O & INC) in MATLAB/Simulink," *Indonesian Journal of Electrical Engineering and Computer Science*, vol. 18, no. 2, Art. no. 2, May 2020, doi: 10.11591/ijeecs.v18.i2.pp666-677.

[20] M. N. Ali, K. Mahmoud, M. Lehtonen, and M. M. F. Darwish, "An Efficient Fuzzy-Logic Based Variable-Step Incremental Conductance MPPT Method for Grid-Connected PV Systems," *IEEE Access*, vol. 9, pp. 26420–26430, 2021, doi: 10.1109/ACCESS.2021.3058052.

[21] S. Necaibia, M. S. Kelaiaia, H. Labar, A. Necaibia, and E. D. Castronuovo, "Enhanced auto-scaling incremental conductance MPPT method, implemented on low-cost microcontroller and SEPIC converter," *Solar Energy*, vol. 180, pp. 152–168, Mar. 2019, doi: 10.1016/j.solener.2019.01.028.

[22] M. H. Anowar and P. Roy, "A Modified Incremental Conductance Based Photovoltaic MPPT Charge Controller," in *2019 International Conference on Electrical, Computer and Communication Engineering (ECCE)*, Feb. 2019, pp. 1–5. doi: 10.1109/ECACE.2019.8679308.

[23] K. W. Nasser, S. J. Yaqoob, and Z. A. Hassoun, "Improved dynamic performance of photovoltaic panel using fuzzy Logic-MPPT algorithm," *Indonesian Journal of Electrical Engineering and Computer Science*, vol. 21, no. 2, Art. no. 2, Feb. 2021, doi: 10.11591/ijeecs.v21.i2.pp617-624.

[24] H. H. H. Mousa, A.-R. Youssef, and E. E. M. Mohamed, "State of the art perturb and observe MPPT algorithms based wind energy conversion systems: A technology review," *International Journal of Electrical Power & Energy Systems*, vol. 126, p. 106598, Mar. 2021, doi: 10.1016/j.ijepes.2020.106598.

[25] M. Kamran, M. Mudassar, M. R. Fazal, M. U. Asghar, M. Bilal, and R. Asghar, "Implementation of improved Perturb & Observe MPPT technique with confined search space for standalone photovoltaic system," *Journal of King Saud University - Engineering Sciences*, vol. 32, no. 7, pp. 432–441, Nov. 2020, doi: 10.1016/j.jksues.2018.04.006.

[26] O. Diouri, N. Es-Sbai, F. Errahimi, A. Gaga, and C. Alaoui, "Modeling and Design of Single-Phase PV Inverter with MPPT Algorithm Applied to the Boost Converter Using Back-Stepping Control in Standalone Mode," *International Journal of Photoenergy*, vol. 2019, p. e7021578, Nov. 2019, doi: 10.1155/2019/7021578.

[27] S. Motahhir, A. El Hammoumi, and A. El Ghzizal, "The most used MPPT algorithms: Review and the suitable low-cost embedded board for each algorithm," *Journal of Cleaner Production*, vol. 246, p. 118983, Feb. 2020, doi: 10.1016/j.jclepro.2019.118983.

[28] D. Khodair, M. S. Salem, A. Shaker, H. E. A. El Munim, and M. Abouelatta, "Application of Modified MPPT Algorithms: A Comparative Study between Different Types of Solar Cells," *Appl. Sol. Energy*, vol. 56, no. 5, pp. 309–323, Sep. 2020, doi: 10.3103/S0003701X20050084.

[29] A. Charaabi, A. Zaidi, O. Barambones, and N. Zanzouri, "Implementation of adjustable variable step based backstepping control for the PV power plant," *International Journal of Electrical Power & Energy Systems*, vol. 136, p. 107682, Mar. 2022, doi: 10.1016/j.ijepes.2021.107682.

[30] A. Bouchaib, R. Taleb, A. Massoum, and S. Mekhilef, "Geometric control of quadrotor UAVs using integral backstepping," *Indonesian Journal of Electrical Engineering and Computer Science*, vol. 22, no. 1, Art. no. 1, Apr. 2021, doi: 10.11591/ijeecs.v22.i1.pp53-61.

[31] K. Ali *et al.*, "Robust Integral Backstepping Based Nonlinear MPPT Control for a PV System," *Energies*, vol. 12, no. 16, Art. no. 16, Jan. 2019, doi: 10.3390/en12163180.

[32] H. Yatimi, Y. Ouberri, S. Chahid, and E. Aroudam, "Control of an Off-Grid PV System based on the Backstepping MPPT Controller," *Procedia Manufacturing*, vol. 46, pp. 715–723, Jan. 2020, doi: 10.1016/j.promfg.2020.03.101.

[33] O. Diouri, N. Es-Sbai, F. Errahimi, A. Gaga, and C. Alaoui, "Control of single phase inverter using back-stepping in stand-alone mode," in *2019 International Conference on Wireless Technologies, Embedded and Intelligent Systems (WITS)*, Apr. 2019, pp. 1–6. doi: 10.1109/WITS.2019.8723761.

[34] A. Ma'arif, M. A. M. Vera, M. S. Mahmoud, S. Ladaci, A. Çakan, and J. N. Parada, "Backstepping Sliding Mode Control for Inverted Pendulum System with Disturbance and Parameter Uncertainty," *Journal of Robotics and Control (JRC)*, vol. 3, no. 1, Art. no. 1, 2022, doi: 10.18196/jrc.v3i1.12739.

[35] D. Zouheyr, B. Lotfi, and B. Abdelmadjid, "Improved hardware implementation of a TSR based MPPT algorithm for a low cost connected wind turbine emulator under unbalanced wind speeds," *Energy*, vol. 232, p. 121039, Oct. 2021, doi: 10.1016/j.energy.2021.121039.

[36] K. Loukil, H. Abbes, H. Abid, M. Abid, and A. Toumi, "Design and implementation of reconfigurable MPPT fuzzy controller for photovoltaic systems," *Ain Shams Engineering Journal*, vol. 11, no. 2, pp. 319–328, Jun. 2020, doi: 10.1016/j.asej.2019.10.002.

[37] T. Dörr, T. Sandmann, and J. Becker, "Model-based configuration of access protection units for multicore processors in embedded systems," *Microprocessors and Microsystems*, vol. 87, p. 104377, Nov. 2021, doi: 10.1016/j.micpro.2021.104377.

[38] L. Belhamel, A. Buscarino, A. Cucuccio, L. Fortuna, and G. Rascona, "Model-Based Design Streamlines for STM32 Motor Control Embedded Software System," in *2020 7th International Conference on Control, Decision and Information Technologies (CoDIT)*, Jun. 2020, vol. 1, pp. 223–228. doi: 10.1109/CoDIT49905.2020.9263910.

[39] D. Pilakkat and S. Kanthalakshmi, "An improved P&O algorithm integrated with artificial bee colony for photovoltaic systems under partial shading conditions," *Solar Energy*, vol. 178, pp. 37–47, Jan. 2019, doi: 10.1016/j.solener.2018.12.008.

[40] V.-Q.-B. Ngo, M. Latifi, R. Abbassi, H. Jerbi, K. Ohshima, and M. khaksar, "Improved krill herd algorithm based sliding mode MPPT controller for variable step size P&O method in PV system under simultaneous change of irradiance and temperature," *Journal of the Franklin Institute*, vol. 358, no. 7, pp. 3491–3511, May 2021, doi: 10.1016/j.jfranklin.2021.02.021.

[41] J. Ahmed and Z. Salam, "A Modified P&O Maximum Power Point Tracking Method With Reduced Steady-State Oscillation and Improved Tracking Efficiency," *IEEE Trans. Sustain. Energy*, vol. 7, no. 4, pp. 1506–1515, Oct. 2016, doi: 10.1109/TSTE.2016.2568043.

[42] K. S. Tey and S. Mekhilef, "Modified incremental conductance MPPT algorithm to mitigate inaccurate responses under fast-changing solar irradiation level," *Solar Energy*, vol. 101, pp. 333–342, Mar. 2014, doi: 10.1016/j.solener.2014.01.003.

[43] R. Kadri, H. Andrei, J.-P. Gaubert, T. Ivanovici, G. Champenois, and P. Andrei, "Modeling of the photovoltaic cell circuit parameters for optimum connection model and real-time emulator with partial shadow conditions," *Energy*, vol. 42, no. 1, pp. 57–67, Jun. 2012, doi: 10.1016/j.energy.2011.10.018.

[44] Z. Zhou, P. M. Holland, and P. Igic, "MPPT algorithm test on a photovoltaic emulating system constructed by a DC power supply and an indoor solar panel," *Energy Conversion and Management*, vol. 85, pp. 460–469, Sep. 2014, doi: 10.1016/j.enconman.2014.06.007.

[45] A. Gaga, Y. Mehdaoui, S. E. Ouahdani, B. E. Hadadi, and F. Errahimi, "Embedded Hardware/Software CAN Node Design for Engineering and Research in the Automotive Application Field," *International Journal on Engineering Applications (IREA)*, vol. 10, no. 2, Art. no. 2, Mar. 2022, doi: 10.15866/irea.v10i2.20813.

[46] S. Arof, N. H. Diyanah, N. M. Yaakop, P. A. Mawby, and H. Arof, "Processor in the Loop for Testing Series Motor Four Quadrants Drive Direct Current Chopper for Series Motor Driven Electric Car," in *Advanced Engineering for Processes and Technologies*, A. Ismail, M. H. Abu Bakar, and A. Öchsner, Eds. Cham: Springer International Publishing, 2019, pp. 59–76. doi: 10.1007/978-3-030-05621-6_5.

[47] B. Fekkak, M. Menaa, A. Loukriz, and A. Kouzou, "Control of grid-connected PMSG-based wind turbine system with back-to-back converters topology using a new PIL integration method," *International Transactions on Electrical Energy Systems*, vol. 31, no. 6, p. e12882, 2021, doi: 10.1002/2050-7038.12882.

[48] M. Errouha, Q. Combe, S. Motahhir, S. S. Askar, and M. Abouhawwash, "Design and processor in the loop implementation of an improved control for IM driven solar PV fed water pumping system," *Sci Rep*, vol. 12, no. 1, Art. no. 1, Mar. 2022, doi: 10.1038/s41598-022-08252-7.

[49] O. Diouri, F. Errahimi, and N. Es-Sbai, "Regulation of the Output Voltage of an Inverter in Case of Load Variation," *IOP Conf. Ser.: Mater. Sci. Eng.*, vol. 353, p. 012021, May 2018, doi: 10.1088/1757-899X/353/1/012021.

[50] O. Diouri, A. Gaga, N. Es-Sbai, and F. Errahimi, "Design and simulation of a novel cascaded transformer multilevel inverter topology for photovoltaic system," in *2015 3rd International Renewable and Sustainable Energy Conference (IRSEC)*, Marrakech, Morocco, Dec. 2015, pp. 1–5. doi: 10.1109/IRSEC.2015.7454957.